Electronic Supplementary Information

Preparation of Fe-based redox couple material

The functional redox material stored in the redox cycle unit consists of a mixture of Fe_2O_3 and ZrO_2 powders in a molar ratio of *ca.* 85:15. The role of ZrO_2 is to mitigate the coarsening of Fe-particles during repeated redox cycles. The nanosize powders of Fe_2O_3 and ZrO_2 were prepared by co-precipitating 0.1 M of aqueous solution containing $Fe(NO_3)_3\cdot 9H_2O$ (Alfa Aeasar, 98.0-101.0%) and $ZrO(NO_3)_2\cdot xH_2O$ (Alfa Aeasar, 99.9%) with $(NH_4)_2CO_3$. The molar ratio was kept as $n_{(NH_4)_2CO_3} : n_{M^{n+}} = 2.5:1$, where M represents the combined Fe and Zr. The obtained co-precipitate was then filtered, washed, dried, ground and finally calcined at 600 ^oC for 2 h to convert it into the oxides. The decomposed oxide powders were then ball-milled to break up the agglomerates, followed by mixing with a microcrystalline cellulose pore-former (type NT-013, FMC Corp.) in a volume ratio of 1:1. The final CLB pellets were made by pressing the powder into Φ1/2" pellets and sintering at 1000^oC for 1 h. All heat treatments were conducted in open air.

Battery assembly

A commercially available anode-supported tubular SOFC (Ni-YSZ/YSZ, CoorsTek) (10 mm in OD, 1.25 mm in wall thickness and 40 mm in length) was used as the core component SOEC in the battery. The resultant effective cell surface area is 4.78 cm^2. A cross-sectional view of the anode/electrolyte microstructure after reduction is shown in Fig.S1, which indicates an approximately 25 μm-thick YSZ electrolyte on the anode with a reasonably good porosity and pore size. The composite cathode ink consisting of GDC ($Ce_{0.8}Gd_{0.2}O_2$) and LSCF ($La_{0.6}Sr_{0.4}Co_{0.2}Fe_{0.8}O_{3-\delta}$) (LSCFGDC-1, Fuel Cell Materials) was applied to the outer surface of the cell and calcined at 1050^{o}C for 1 h in open air. The currents were collected by silver wires attached on the outer surface of the cathode and one end of the anode as shown in Fig.S2. To ensure good electrical contacts, a layer of silver prepared from silver paste (C8829, Heraeus) was coated prior to attaching the silver wires. Served as the transitional part, two Al_2O_3 rings were attached to the two ends of the cell. The battery cell was finally cement-mounted onto two long Al_2O_3 tubes in which Fe_2O_3-ZrO_2 pellets were installed close to the inlet end of the battery cell. After a full reduction, the Fe loading is determined to be 0.1064 grams from initial Fe_2O_3/ZrO_2 loading, due to limited space in our lab-scale battery prototype. The volume of the enclosed loop in the fabricated battery cell is approximately 81.5 cm^3. Fig.S3 shows a schematic view of the assembled battery cell.

Test setup and methodology

Fig.S4 shows the flow block diagram of the battery test setup. Overall, it consists of three major components: the battery cell, circulating pump, and a set of toggle valves. By turning off and on certain toggle valves, a closed-loop circulation can be created by the pump. The flow rates of all the gases used (N_2, H_2 and Air) were controlled by the mass flow controllers (MFCs). The desirable H_2O contents were obtained by passing the carrier gas N_2 or H_2 through a bubbler heated to a fixed temperature. An on-line humidity sensor (Vaisala model 332) was deployed to measure the real-time steam content in the gas phase. To prevent condensation, all pipelines were heat-wrapped and kept at 150^oC. A Solartron 1260/1287 Electrochemical System (not shown in Fig.S4) was employed to measure the electrical performance of the battery with software modules such as OCV (open circuit voltage)-t, impedance spectroscopy, potential-dynamic and galvanic square wave.

A typical characterization procedure can be described as follows. Pure N_2 is first used to purge the entire pipe system several times to remove any possible residual air in the circulation loop. The battery is then heated up to the target temperature of 800^oC with a ramp rate of 3^oC/min and 200-sccm air and 90-sccm 5%H_2-N_2 flowing outside and inside of the battery cell, respectively. During this period, the open-circuit voltage is constantly monitored while NiO in the anode and Fe_2O_3 in the redox cycle unit are being at least partially reduced. After reaching 800^oC, 5%H_2-N_2 is then gradually switched to 90 sccm dry H_2 to complete the reduction of all Fe_2O_3 into Fe, which becomes the starting point of each battery test. Nitrogen is the primary carrier gas for bringing the steam into the redox cycle unit where oxidation of Fe takes place, producing H_2 for the discharge cycle. At each H_2O concentration, OCV-t, impedance spectroscopy, V-I characteristic and galvanic square wave are conducted before H_2 is introduced to reduce the oxidized Fe back to Fe for the next-round characterization. To ensure no H_2 is left in the pipeline, H_2O-bore N_2 is allowed to purge through for 1 minute (obviously some produced H_2 could be lost during the purge) before the measurement starts. Upon circulation, the outlet and inlet toggle valves are sequentially shutoff, immediately followed by turning on the pump. The pump was set to a pre-calibrated flow rate of 90 sccm N_2-flow.

Fig.S5 shows charge/discharge curves recorded in a stagnant gas. Evidently, after just a few cycles, the battery performance decayed rapidly, particularly for the charging cycle, indicating the importance of dynamic flow of the gas phase.

Thermodynamic analysis

The chemical compositions of H_2-H_2O and N_2-H_2O mixtures equilibrated with Fe and FeO at 800°C were analyzed with HSC Chemistry software (Outokumpu Research Oy) and are plotted in Fig.S6. For N_2-H_2O inlet gas, Fig.S6 (a), the equilibrium composition features a constant H_2/H_2O ratio of 65.1:34.9. The higher the H_2O content in the inlet gas, the more H_2 is produced. For H_2-H_2O inlet gas, Fig.S6 (b), any composition higher than H_2/H_2O=65.1/34.9 will maintain its original gas composition, *i. e.*, Fe is not oxidizable at this condition whereas any composition lower than H_2/H_2O=65.1/34.9 will be equilibrated at the constant H_2/H_2O=65.1/34.9 ratio.

Fig.S7 shows the E_N as a function of pH_2O/pH_2 at 800°C. With the calculated pH_2O/pH_2 for both Fe-FeO and FeO-Fe_3O_4 equilibria, for example, the E_N values are 0.970 and 0.938 volts, respectively. The observed E_N= 0.970 volt during the battery testing is a clear indication of Fe-FeO equilibrium being a stable redox-couple in the redox cycle unit.

Fig.S8 compares (a) Nernst potential E_N and (b) specific energy density (SED) among several transition metal-oxide redox-couples at different temperatures. Clearly, the redox couples containing metals with a greater oxygen affinity exhibit higher E_N and SED because of the higher ($-\Delta G$) values.

Calculations of energy capacity and Fe utilization

The total charge stored in Fe, full discharge time, and Fe utilization are, respectively, estimated from the following equations:

$$\text{Total charge } Q^*_{Fe} \text{ (Coulomb) stored in Fe: } Q^*_{Fe} = \frac{W_{Fe}}{M_{Fe}} \times 2 \times F \qquad \text{(S1)}$$

$$\text{Full discharge time } t^{*}_{\mathrm{Fe}} \text{ (sec): } t^{*}_{\mathrm{Fe}} = \frac{Q^{*}_{\mathrm{Fe}}}{I_{\mathrm{d}}} \qquad \text{(S2)}$$

$$\text{Fe utilization } U_{\mathrm{Fe}}\text{: } U_{\mathrm{Fe}} = \frac{Q_{\mathrm{Fe}}}{Q^{*}_{\mathrm{Fe}}} = \frac{t_{\mathrm{Fe}}}{t^{*}_{\mathrm{Fe}}} \qquad \text{(S3)}$$

where W_{Fe} (g) and M_{Fe} (g/mole) are the actual weight and atomic weight of Fe, respectively; I_d is the galvanic discharge current in amperes; Q_{Fe} and t_{Fe} are the measured charge capacity (Coulomb) and actual cycle time (seconds), respectively. At 50 mA/cm^2 (or 0.239 A with an effective cell surface area of 4.78 cm^2 used in this study), the full discharge time for 100% utilization of 0.1064 gram of Fe is roughly 26 minutes. A 10-minute discharge cycle shown in Fig. 4 infers 38.5% of Fe utilized during the discharge cycle.

Figure captions

Fig.S1 Cross-sectional microstructural view of an anode-supported tubular SOEC employed in this study

Fig.S2 A single battery cell subassembly

Fig.S3 A single battery assembly with an integrated redox-cycle unit

Fig.S4 A flow block diagram of test configuration for the battery

Fig.S5 Charge and discharge characteristics of the battery measured at 800°C and J=50 mA/cm^2 in a closed stagnant gas of 53.2%H_2O-N_2. Single-cycle period is 10-minute.

Fig.S6 Calculated equilibrium gas compositions of (a) N_2-H_2O and (b) H_2-H_2O systems reacting with Fe and FeO at 800°C

Fig.S7 Calculated Nernst potential as a function of pH_2O/pH_2 at 800°C

Fig.S8 Comparison of E_N (a) and specific energy density (SED) (b) among several transition metal-oxide redox-couples at different temperatures

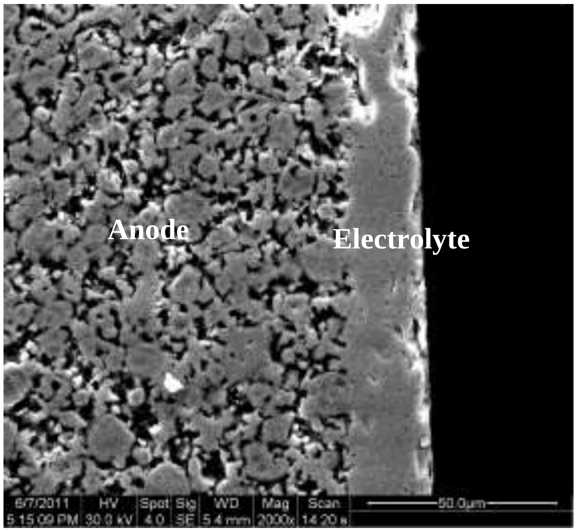

Fig.S1 Microstructure of an anode-supported tubular SOEC employed in this study

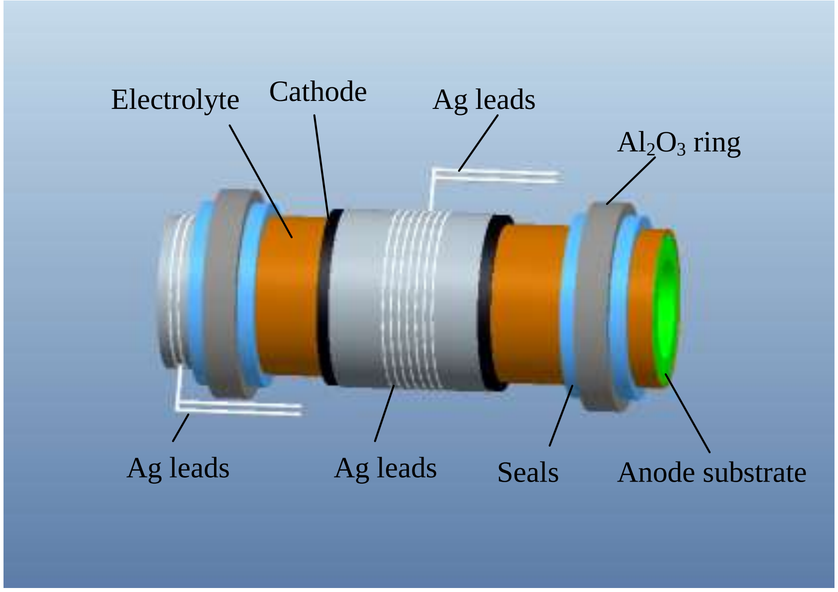

Fig.S2 A single battery cell subassembly

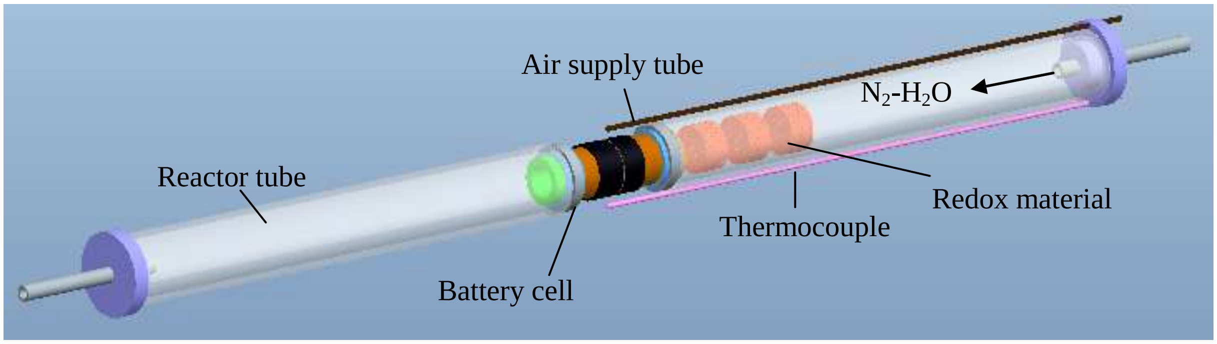

Fig.S3 A single battery assembly with an integrated redox-cycle unit

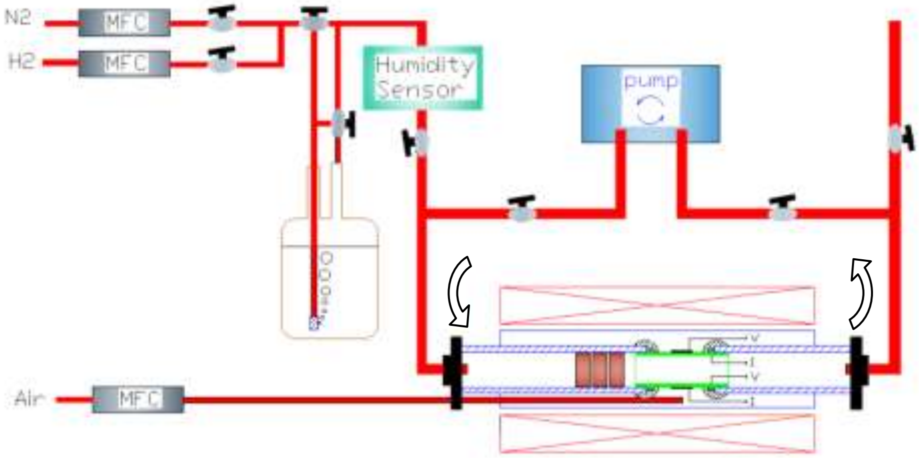

Fig.S4 A flow block diagram of test configuration for the battery

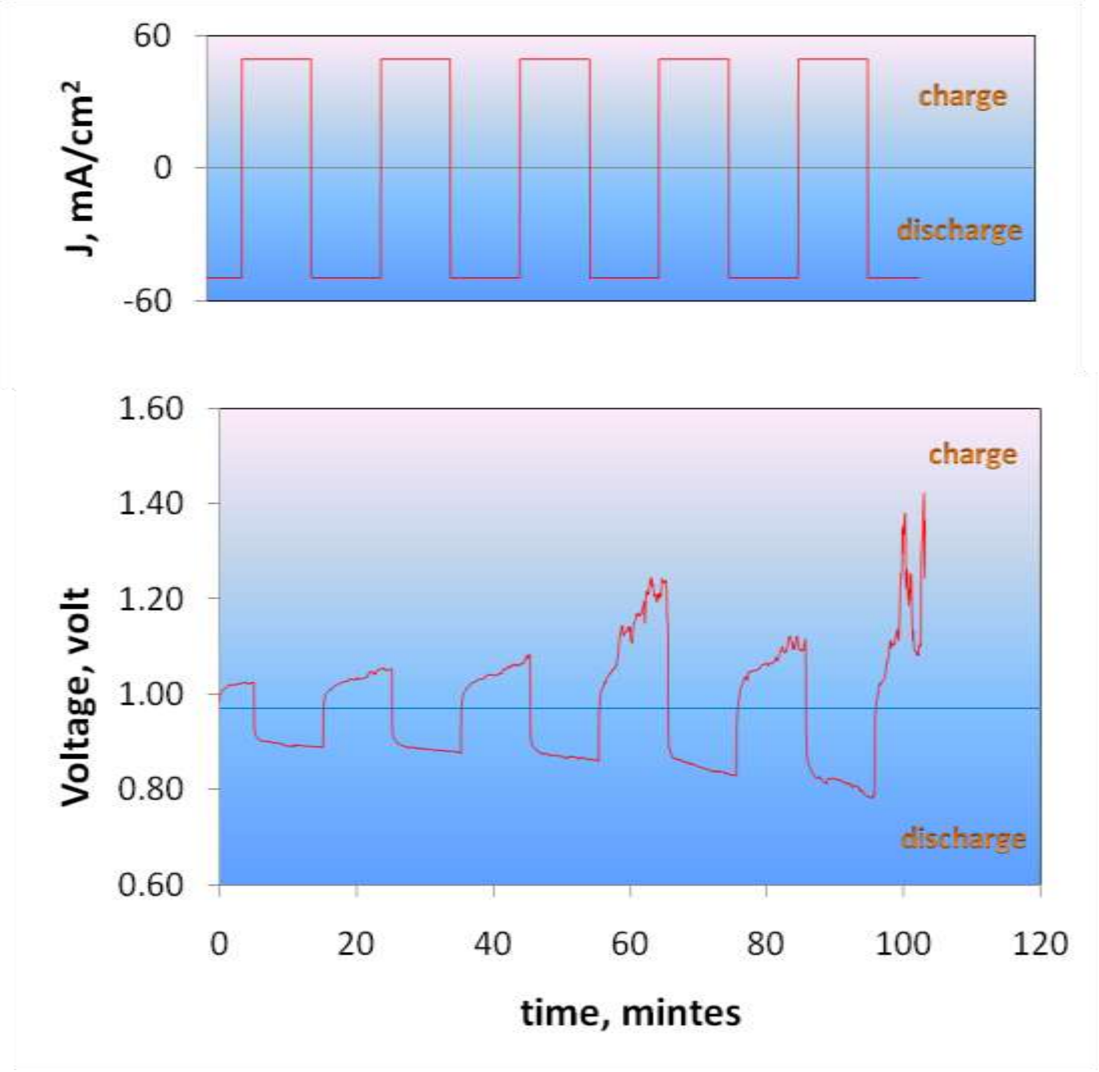

Fig.S5 Charge and discharge characteristics of the battery measured at 800^{o}C and J=50 mA/cm^{2} in a closed stagnant gas of 53.2%H_2O-N_2. Single-cycle period is 10-minute.

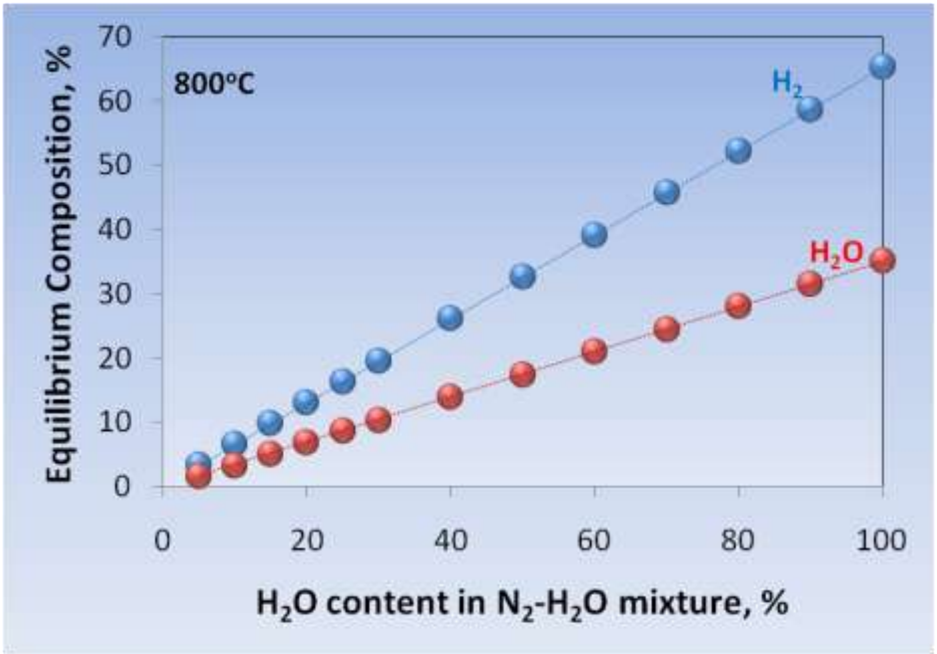

(a)

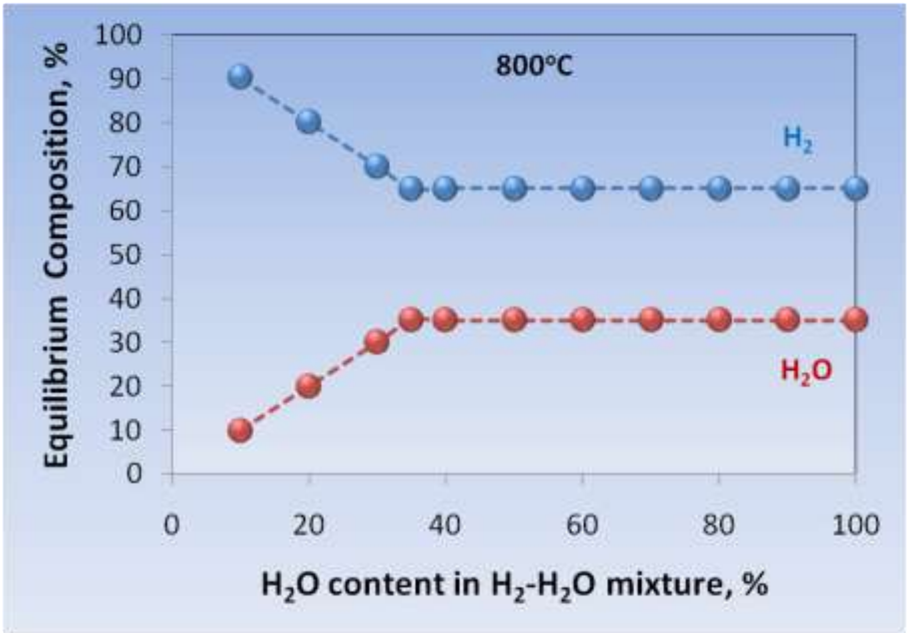

(b)

Fig.S6 Calculated equilibrium gas compositions of (a) N_2-H_2O and (b) H_2-H_2O systems reacting with Fe and FeO at 800°C

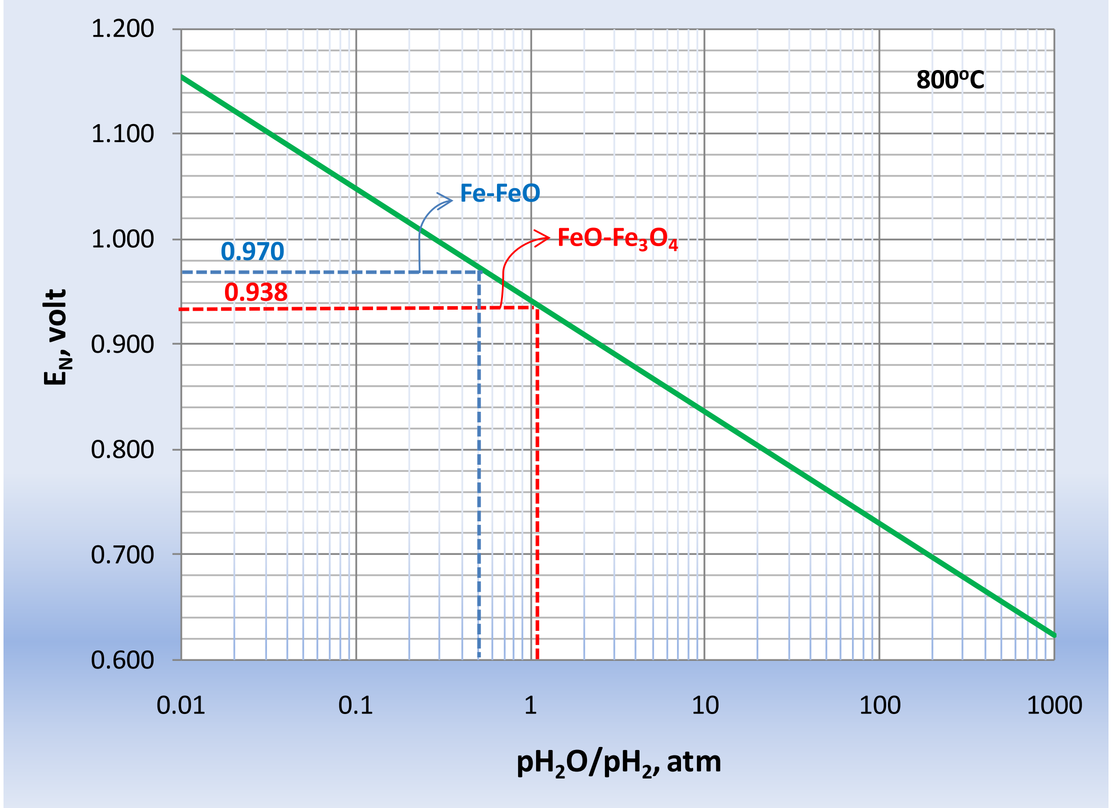

Fig.S7 Calculated Nernst potential as a function of pH_2O/pH_2 at 800^oC

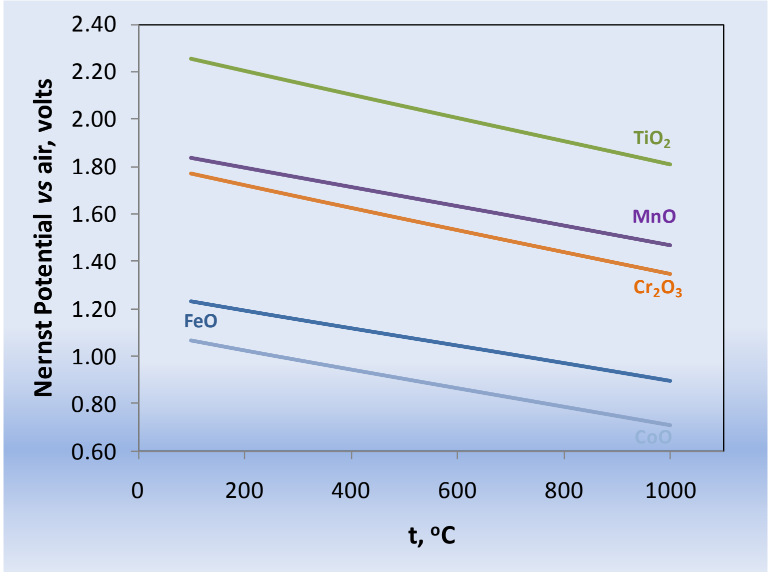

(a)

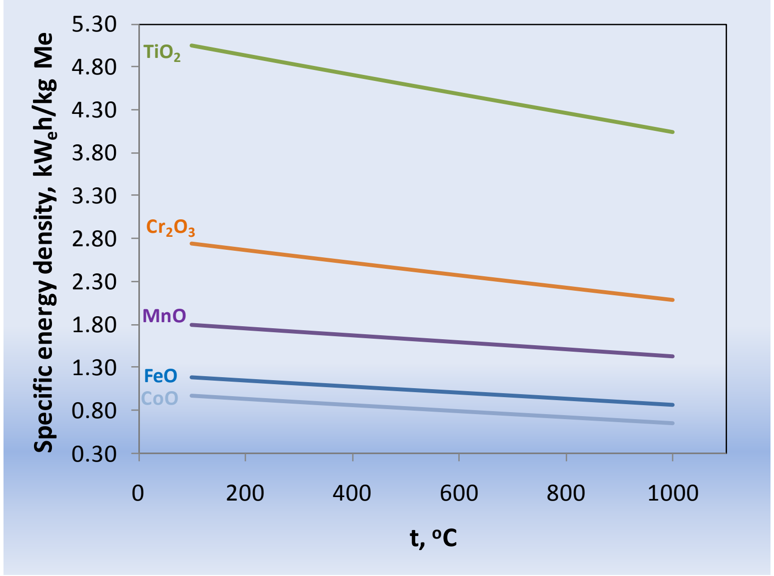

(b)

Fig.S8 Comparison of E_N (a) and specific energy density (SED) (b) among several transition metal-oxide redox-couples at different temperatures